Jurnal Sains Materi Indonesia
Indonesian Journal of Materials Science

Edisi Khusus Oktober 2007, hal : 88 - 94
ISSN : 1411-1098

Akreditasi LIPI Nomor : 536/D/2007
Tanggal 26 Juni 2007

THE STRUCTURAL AND MICROSTRUCTURAL CHARACTERISTICS IN THE MILLED $Fe_{50}C_{50}$ MAGNETIC COMPOSITES

Setyo Purwanto and Engkir Sukirman
Center for Technology of Nuclear Industry Materials (PTBIN)-BATAN
Kawasan Puspiptek Serpong 15314, Tanggerang

ABSTRACT

THE STRUCTURAL AND MICROSTRUCTURAL characteristics IN THE MILLED $Fe_{50}C_{50}$ MAGNETIC COMPOSITES. The structural and microstructural characteristics in the milled $Fe_{50}C_{50}$ magnetic composites have been investigated by the x-ray diffraction technique using Rietveld analysis method. The starting materials of composite were the pure iron (Fe) and carbon (C) powders (weight ratio Fe:C = 50:50). The composites were prepared by mixing Fe and C powders by high energy milling (HEM) at various milling time start from 1.5 to 4.5 h. The x-rays diffraction measurements were performed by using a Philips X-Ray Diffractometer, PW170 type at room temperature with CuKα radiation, 2θ range = 10°-100°, preset time = 1 sec, and step size = 0.020°. With a mechanical milling of 4.5 hours, the elemental powders undergo a better crystallization. It means that the amorphization. Of its components do not happen yet. The carbon elements in composites get a homogeneous strain field, while the iron elements get an inhomogeneous strain field. The crystallite size of C particles almost do not change yet until the milling time of 4.5 hours. This is presumably due to the C particles are trapped at the weld interfaces between the Fe particles. While, the Fe particles fracture into smaller segments on the milling time of 1.5 hours. On the further milling, the Fe particles undergo welding processes to be bigger crystallites. Magnetic parameter such as Hc,Ms and Ku were confirmed this suggestion.

Key words : Mechanical milling, $Fe_{50}C_{50}$ composite, X-ray diffraction, Rietveld method.

ABSTRAK

SIFAT-SIFAT STRUKTUR DAN MIKROSTRUKTUR KOMPOSIT MAGNET $Fe_{50}C_{50}$ HASIL *MILLING*. Sifat-sifat struktur dan strukturmikro komposit bahan magnetik $Fe_{50}C_{50}$ hasil *milling* telah diteliti dengan teknik difraksi sinar-X metode analisis *Rietveld*. Bahan baku komposit adalah serbuk besi (Fe) dan karbon (C) murni (perbandingan berat Fe:C=50:50). Komposit dibuat dengan mencampurkan serbuk Fe dan C menggunakan *High Energy Milling* (*HEM*) dengan waktu *milling* divariasi mulai dari 1,5 hingga 4,5 jam. Pengukuran difraksi sinar-x dilakukan menggunakan Difraktometer Sinar-X Philips, model PW170 pada suhu kamar, radiasi = CuKα, daerah 2θ = 10° hingga 100°, *preset time* = 1 detik, dan lebar langkah = 0,020°. Dengan *milling* selama 4,5 jam, unsur Fe dan C mengalami kristalisasi lebih baik, artinya belum terjadi amorfisasi. Unsur karbon di dalam komposit terkena medan regangan homogen, sedangkan unsur besi mendapat regangan tidak homogen. Ukuran kristalit partikel-partikel C hampir tidak berubah hingga *milling* 4,5 jam. Hal ini mungkin karena partikel-partikel C terperangkap pada antarmuka patrian diantara partikel-partikel Fe. Sedangkan partikel-partikel Fe terbelah menjadi partikel yang lebih kecil setelah *milling* 1,5 jam. Pada *milling* selanjutnya, partikel-partikel Fe mengalami proses pematrian sehingga menjadi kristalit yang lebih besar. Besaran parameter magnetik seperti Hc,Ms dan Ku terlihat memperkuat kesimpulan tersebut.

Kata kunci : *Mechanical milling*, Komposit $Fe_{50}C_{50}$, Difraksi sinar-X, Metode *Rietveld*.

INTRODUCTION

It is fascinating to investigate the materials containing carbon element or carbon based materials. Although carbon is only light element but having a wide spread industrial applications. This is partly because carbon have many forms in terms of structure configuration. Recent experiments reveal that even in pure highly oriented pyrolytic graphite, ferromagnetism and superconductivity properties can exist [1]. Many research works have revealed the superconductivity in alkali doped C_{60} such as in M_3C_{60}(S) (M = K, Rb, Cs and various mixures of alkali atoms), M_5C_{60}(S) (M = Ca) [2], and also in the graphite composite materials [3].

Those findings have triggered renewed investigation on carbon based materials. One of the

investigations was conducted [4]. They have found a large positive magnetoresistance (MR) in micro-size Fe_x-C_{1-x} composites. In their experiment, the samples of micrometer particle Fe-C composites were prepared using a kind of heat-pressure system. Every specimen under study has a linear field dependence of the positive MR at different temperatures, and therefore they can design different magnetic sensors to satisfy different demands using Fe-C composites. Thus, iron which is a ferromagnetic material, when it is made as composite of carbon, changes its properties into the magnetic materials that exhibiting large magnetoresistance (MR). The results imply that the structure dimension or topology may play some fundamental role in figuring out the physical properties of Fe-C composites [1]. Another way in designing, modifying, tailoring the crystal structure, and the microstructure and consequently the physical properties of matter is by means of High Energy Milling (HEM).

The effect of order-disorder developed in the high energy milling process can result in the crystal structure, and the microstructure defects and cause the appearance of magnetic properties induced by structural instability. This topological defects may lead to the magnetoresistance of Fe-C composites. In addition, the crystal structure, and the microstructure defects may result in the lattice strain, and the residual stress in matters. The present investigation was undertaken the Rietveld analysis based on x-ray powder diffraction patterns to determine the structural and microstructural characteristics of the Fe-C magnetic composites prepared by the high energy milling.

X-ray and neutron diffraction are powerful nondestructive techniques for characterizing residual stresses in crystalline materials [5]. When a material is subject to a homogeneous strain field, the angular position of a diffraction peak will shift to lower or higher 2θ values, depending on whether the strain is tensile or compressive. If the material is subject to an inhomogeneous strain field, then in addition to a peak position shift as mentioned above, the diffraction peak profile will also be broadened. Thus, the shift of a peak measures the average lattice strain along a particular crystallographic direction. While, the peak broadening can be ascribed to either a small particle size or an inhomogeneous strain field, or both. Typically the broadening due to a small particle size appears in the form of a Lorentzian whereas that due the inhomogeneous strain field is described by a Gaussian function. From the experimentally determined strains, the residual stresses can be deduced using appropriate models [6].

By using the Rietveld analysis method, the precision of the strain measurements can be further improved. In a Rietveld analysis, structure parameters calculated for every phases in a composite sample can be determined very accurate although there are many overlap reflections. In a Rietveld analysis, the parameters in a structural model, plus necessary instrumental parameters, are adjusted in a computer calculation until the least-squares best fit is obtained between the entire calculated and observed powder patterns. Since a large number of diffraction peaks are fitted simultaneously, the statistical errors introduced in individual peak fitting are largely reduced. Moreover, by fitting to the whole pattern, any effects of preferred orientation, extinction, and other systematic aberrations, if present, will also be minimized [7]. Accordingly, the maximum amount of information can reliably be derived from the observed intensity data. Therefore, this technique has now found wide spread application in the structure determination of compounds which are not available as single crystals.

THEORY

Crystallites are coherent (free of defects) crystal units that diffract in phase. The term crystallite size is commonly substituted for the term grain size when related to metallic films. The crystallite size is only equivalent to grain size if the individual grains are perfect single crystals free of defects, grain boundaries, or stacking faults.

Crystallite size is determined by measuring the broadening of a particular peak in a diffraction pattern associated with a particular planar reflection from within the crystal unit cell. It is inversely related to the FWHM (full width at half maximum) of an individual peak-the more narrow the peak, the larger the crystallite size. If the crystals are defect free and periodically arranged, the x-ray beams are diffracted to the same angle, in phase, and reinforcing each other even through multiple layers of specimen, resulting in a tall narrow peak. If the crystals are randomly arranged or have low degrees of periodicity, the result is a broader peak.

The broadening of a diffraction peak due to the presence of an inhomogeneous strain field is given by [8]

$$B^2 = B_0^2 + 32 \ln 2 . \tan^2 \theta . e_{hkl}^2 \quad \text{..... (1)}$$

where B is the FWHM of the broadened peak and B_0 is the instrumental resolution which varies with θ according to the Cagliotti equation [9]

$$B_0^2 = U_0 \tan^2 \theta + V_0 \tan \theta + W_0 \quad \text{..... (2)}$$

A simpler approach is taken to obtain an estimate of $<e>$, the average value of the anisotropic *rms* strains within the composites. Substituting Eq.(2) into Eq.(1), we have

$$B^2 = (U_0 + 32 \ln 2 . < e_{hkl}^2 >) \tan^2 \theta + V_0 \tan \theta + W_0$$

$$= U \tan^2 \theta + V_0 \tan \theta + W_0 \quad \text{..... (3)}$$

Edisi Khusus Oktober 2007, hal : 88 - 94
ISSN : 1411-1098

where $U = (U_0 + 32\ln 2. < e_{hkl}^2 >)$; so from this equation, we have

$$< e_{hkl}^2 >= \frac{U - U_0}{32\ln 2} \quad \text{..... (4)}$$

where U is the FWHM parameters of the broadened peak due to the presence of an inhomogeneous strain field and U_0 is the one due to the instrumental resolution only.

The crystallite size calculations are determined using the Scherrer equation [10]:

$$\beta(\frac{\cos\theta}{\lambda}) = 2\eta(\frac{\sin\theta}{\lambda}) + \frac{0{,}9}{D} \quad \text{…….....……...… (5)}$$

where β = full width at half maximum (FWHM), η = lattice strain, θ = Bragg peak angle, λ = wave length (usually 1.54056 ï for Cu Kα_1 radiation), and D = crystallite size. So, the Scherrer equation yields the crystallite size and lattice strain for a specific peak or reflection. Therefore, to obtain a more general idea of the overall crystallite size and lattice strain, an average crystallite size and lattice strain are determined using multiple peaks.

Now that the lattice strains have been characterized, the residual stresses in each phase can be deduced. In fact, the average lattice strains discussed above, which were obtained from the refinement of a diffraction pattern over a wide angular range and hence represented some kind of average over many directions in the diffraction plane, are a better measure of the hydrostatic stress rather than the stress along a particular sample orientation. The hydrostatic stress, σ, is related to the hydrostatic strain, ε, by the following equation [11].

$$\sigma = \frac{E}{1-2\nu}\varepsilon \quad \text{…….....……... (6)}$$

where E is Young's modulus and ν is Poisson's ratio of the specific material considered and in this case, ε replaced by $<e_{hkl}>$ parameters. The E parameters and ν used in the evaluation of σ were obtained from independent mechanical measurements, i.e. for iron, E = 206.4 GPa, ν = 0.34 and for carbon, E = 25.5 GPa, ν = 0.31 [12,13].

EXPERIMENTAL METHOD

Sample Preparation

Starting materials for the preparation of $Fe_{50}C_{50}$ magnetic composite were the pure iron (Fe) and carbon (C) powders (weight % of Fe:C = 50:50). The Fe-C magnetic composites were prepared by mixing Fe and C powders by High Energy Milling (HEM) [14] to synthesize nanocrystalline $Fe_{50}C_{50}$ composite. The total weight of powders milled is 2 g. The main event in HEM is the ball-powder-ball collision. Powder particles are trapped between the colliding balls during milling. The powders milled then undergo microscopic deformation and/or fracture processes and welding which result ultimate structure of the powder. These collisions in turn are influenced by the macroscopic parameters which differ in the various mill types as well as milling media size (total ball mass), powder mass ratio, and milling time.

In this experiment we introduced five of steel balls into the vial where the weight of each ball is 7 ~ 8 g. Thus, the total ball mass and powder mass ratio is 1.8:1. The milling time of the samples were varied of 1.5, 2.0, 2.5, 3.0, 3.5, 4.0, and 4.5 hour; so we have seven composite samples called then FEC1.5, FEC2.0, FEC2.5, FEC3.0, FEC3.5, FEC4.0, and FEC4.5, respectively.

X-Ray Diffraction and M-H Curve Measurements

The phases analysis on the seventh composite samples along with the two of Fe and C powder pure samples were carried out qualitatively and quantitatively by x-rays diffraction technique using the Rietveld method [15]. The x-rays diffraction experiments were performed by using a Philips X-Ray Diffractometer, PW170 type. The x-ray intensity data from every point were collected at room temperature with CuKα radiation for 1 sec from 10° to about 100° in 2 at a step size of 0.020°.

While, the magnetic properties of the samples were measured by VSM (*Vibrating Sample Magnetometer*). All of these experiments were carried out at the Laboratory of the Characterization and Nuclear Analysis, Technology Center for Nuclear Industrial Materials, National Nuclear Energy Agency, Puspiptek, Setu, Tangerang, Banten.

Structural Refinements

The obtained diffraction data were analyzed using RIETAN, a Rietveld structure refinement program developed by Izumi [15]. The angular coverage of the experimental data was adequate to allow the structural parameters for each phase to be refined. This include the lattice parameters, the atomic coordinates, and the isotropic thermal parameters. The background correction Y_{bi} was modeled using the six-parameter function

$$Y_{bi} = \sum_{j=0}^{5} b_j [\frac{2\theta_i}{(\theta_{\max} - \theta_{\min})} - 1]^j \quad \text{…….....…….....} (7)$$

where b_o-b_5 are the background parameters, and θ_{max} and θ_{min} are respectively the maximum and minimum values of diffraction angles in step scanned intensity data. The x-ray powder diffraction patterns of the two samples were presumed to contain only the peaks of Fe and C phases.

RESULT AND DISCUSSION

As mentioned above that the diffractometer used to measure the sample can also introduce a small amount of peak broadening purely as a function of the electronic and mechanical interactions. This inherent broadening is called instrumental broadening. In this experiment, the instrumental broadening was measured by using a Si-standard sample. The Rietveld refinement patterns for the Si phase is indicated in Figure 1 and the FWHM parameters are indicated in Table 1. In the upper portions of the figure here and elsewhere, the observed data are indicated by the dots; the calculated patterns are showed as the solid line overlying them. The vertical makers in the central portions show positions calculated for $K\alpha_1$ and $K\alpha_2$ peaks. The lower portions are plots of Δ, the difference between the observed and calculated intensities. It is clearly indicated that the full powder patterns calculated from the refined parameters matched the experimental patterns.

Table 1. The Full Width at Half Maximum (FWHM) parameters of Si crystal, where U_0 = -0.00284(3), V0 = 0.00090(4), W_0 = 0.001060(8), and lattice parameters: a = b = c = 5.4326(2) ú.

Parameters	(*hkl*)					
	[111]	[220]	[311]	[222]	[400]	[331]
2θ	28.433	47.286	56.102	58.835	69.104	76.347
FWHM (º)	0.1164	0.1309	0.1368	0.1384	0.1437	0.1464

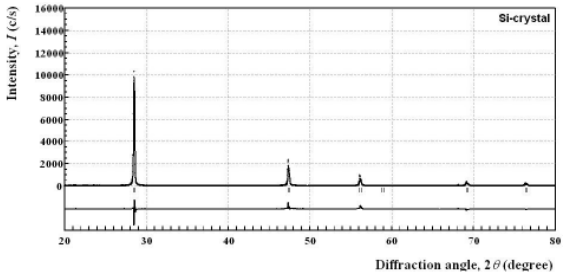

Figure 1. Rietveld refinement patterns of x-rays diffraction for the Si crystal with the S factor of 1.7026.

The Fe phase were assumed to crystallize into crystal system: cubic, space group: Im3m (Vol. I, 29), equivalent position for each site: [0,0,0] and (1/2,1/2,1/2), lattice parameters: $a = b = c = 2.86190$ ú, and $\alpha = \beta = \gamma = 90º$. While C phase were considered to have a crystal system: hexagonal, space group: P63/mmc (Vol. I, 194), equivalent position for each site: (0,0,1/4) and (1/3,2/3,1/4), lattice parameters: $a = b = c = 2.86190$ ú, and $\alpha = \beta = 90$, $\gamma = 120º$. Rietveld refinement patterns for the Fe and the C phases are showed in Figure 2 and Figure 3, respectively. On the two figures are clearly showed that the full powder patterns calculated from the refined parameters matched the experimental patterns. These results support the ideas that each of the Fe and C phases have the structural parameters as mentioned above, and the *S* factors are showed in Table 2.

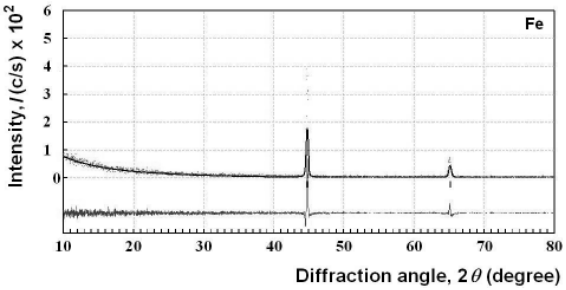

Figure 2. Rietveld refinement patterns for the Fe (iron) phase. There are two peaks detected, i.e. [110] and [200] on 2θ positions of 44.747° and 65.137°, respectively.

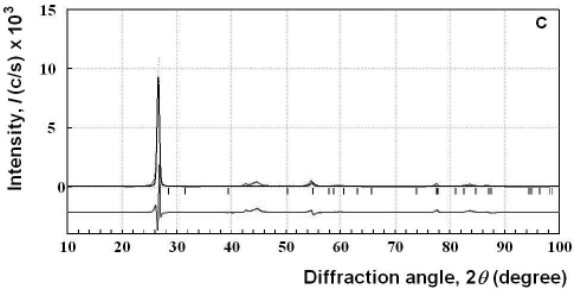

Figure 3. Rietveld refinement patterns for the C (carbon) phase. There is one highest peak detected, i.e. [002] on on 2θ position of 26.634°.

Rietveld refinement patterns for the FEC1.5, FEC2.0, FEC2.5, FEC3.0, FEC3.5, FEC4.0, and FEC4.5 samples are indicated on the Figure 4 (a), (b), (c), (d), (e), (f), and (g). The experimental data are plotted by dots, and the solid curve overlying the data dots is a diffraction pattern calculated from the final parameters. The Rietveld refinements for the seven samples converged most satisfactory, giving quite-low S factors (Table 2), where *S* is the goodness of fitting indicator. The standard value for *S* is 1.30 [15], the smaller the S factor, the better the fitting quality is. It is clearly indicated in the Table 2 that the *S* values decrease by increasing the milling time. It means that the fitting quality is getting better on the samples with a longer time of milling. In other word, the calculated patterns matched the experimental one more closely on the samples with a longer milling period. These results show that the samples only containing two phases, i.e. iron and carbon. There are no contamination which may arise from the milling media and atmosphere, and the alloying of Fe and C did not occur during milling. From this fact is concluded that high energy milling of $Fe_{50}C_{50}$ composites for 4.5 hours result in a better crystallization of component powders.

The [002] Bragg-peak position of carbon shifts to lower value as clearly indicated in Table 2, and Figure 5, but the full width at half maximum (β) almost does not change with increasing the milling time. As β almost does not change, then the crystallite size (*D*) also almost fix at the same value with increasing the milling time as indicated in Table 3, where *D* has an average value of 223 Å. This is because of the full width at half maximum

Edisi Khusus Oktober 2007, hal : 88 - 94
ISSN : 1411-1098

Table 2. The full width at half maximum (FWHM), Bragg angle (2θ) data, and the S factors.of $Fe_{50}C_{50}$ magnetic composites samples.

No.	Sample	FWHM (β)		Bragg Angle (2θ)		*S* Factors
		Fe phase $\beta_{(110)}$ (°)	C phase $\beta_{(002)}$ (°)	Fe phase $2\theta_{(110)}$ (°)	C phase $2\theta_{(002)}$ (°)	
1.	FE	0.3548	-	44.747	-	3.997
2.	C	-	0.5045	-	26.634	1.156
3.	FEC1.5	0.3856	0.4063	44.744	26.672	1.684
4.	FEC2.0	0.3387	0.3502	44.705	26.612	1.614
5.	FEC2.5	0.3354	0.3497	44.702	26.600	1.452
6.	FEC3.0	0.2469	0.3571	44.628	26.505	1.287
7.	FEC3.5	0.3027	0.3803	44.663	26.528	1.206
8.	FEC4.0	0.2058	0.3784	44.645	26.496	1.060
9.	FEC4.5	0.1961	0.3987	44.619	26.458	1.080

of an individual peak is straightly related to the crystallite size. From those data, we can deduce that the carbon elements in $Fe_{50}C_{50}$ magnetic composites get a homogeneous strain field, and according to Xun-Li Wang *et al* [6], the type of its strain field must be tensile.

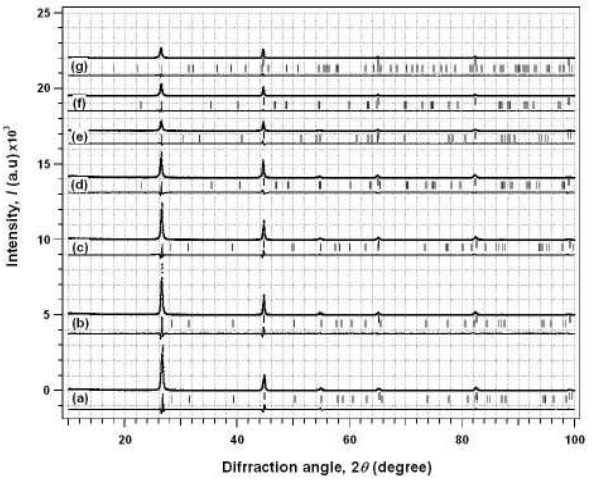

Figure 4. Rietveld refinement patterns for the FEC1.5 (a), FEC2.0 (b), FEC2.5 (c), FEC3.0 (d), FEC3.5 (e), FEC4.0 (f), and FEC4.5 (g) samples.

The [110] Bragg-peak position of iron also shifts to lower value as clearly indicated in Table 2, and Figure 6. In addition to a peak position shift, however, the diffraction peak profile is getting narrower and so also β. As β is getting narrower, then *D* is being bigger with increasing the milling time as indicated in Table 3, where *D* increase to a value of 665 Å from 426 Å. It means that the iron elements in $Fe_{50}C_{50}$ magnetic composites synthesized by HEM get an inhomogeneous strain field.

An interesting question is why the crystallite size of C tends to be no change and even for Fe tends to have a larger crystallite size, after 4.5 hours milling time. The central event in HEM is the ball-powder-ball collision. Powder particles are trapped between the colliding balls during milling and undergo microscopic deformation, welding, and/or fracture processes which define the ultimate structure of the powder [14]. The nature of these processes depends upon the mechanical behavior of the powder components, their phase equilibria, and the stress state during milling. In particular, component powders that are (1) both ductile,

Table 3. Average crystallite sizes, D; lattice strains, <e>; and residual stresses, σ each for Fe and C phases.

No.	Sample	Average Crystallite Sizes, *D*		Average Lattice Strains, $<e_{hkl}>$		Average Residual Stresses, σ	
		Fe phase *D*(?)	C phase *D*(?)	Fe phase $<e_{hkl}>$ (%)	C phase $<e_{hkl}>$ (%)	Fe phase σ (GPa)	C phase σ (GPa)
1.	FE	426	-	0.0603	-	38.908	-
2.	C	-	137	-	0.0434	-	2.915
3.	FEC1.5	343	188	0.0484	0.0850	31.239	5.703
4.	FEC2.0	446	231	0.0507	0.0964	32.683	6.469
5.	FEC2.5	457	231	0.0508	0.0967	32.785	6.492
6.	FEC3.0	501	307	0.0739	0.1243	47.655	8.344
7.	FEC3.5	597	204	0.0513	0.0952	33.105	6.392
8.	FEC4.0	629	256	0.0727	0.1292	46.921	8.668
9.	FEC4.5	665	232	0.0716	0.1301	46.176	8.729

(2) ductile/brittle, or (3) both brittle, exhibit different morphologies during milling.

According to C.C. Koch and J. D. Whittenberger [14], in ductile/brittle powder mixtures (like Fe/C), the brittle particles fracture are trapped at the weld interfaces between ductile particles. The continued fracture and cold-welding ultimately results in a uniform distribution of the brittle particles in the ductile matrix. In this experiment, the C particles are brittle powders and do not fracture yet because they are trapped at the weld interfaces between the Fe particles, in such a way that the crystallite size of C particles do not change yet until the milling time of 4.5 hours. While, the Fe particles which are ductile powders, fracture from a crystallite size of 426 Å into smaller segments (*D* = 343 Å) on the milling time of 1.5 hours. However on the further milling, the Fe particles undergo welding processes. So we get ultimate structure of the Fe particles with a bigger crystallite size (*D* = 665 ú) as indicated in Table 3.

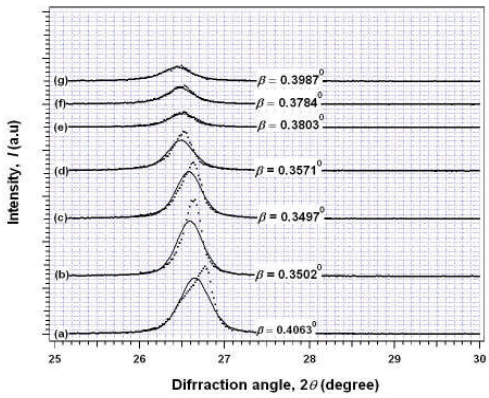

Figure 5. The [002] peak position of carbon phase shifts to lower value, and b value almost does not change on (a) through (d) curve.

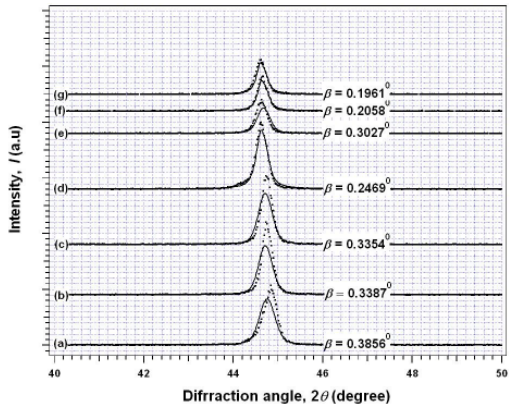

Figure 6. The (110) peak position of iron phase shifts to lower value but b value is getting smaller on (a) through (g) curve.

The lattice strains, $<e_{hkl}>$ of Fe-, and C-phases in the $Fe_{50}C_{50}$ composites were determined by using Equation (4). While the crystallite sizes, *D* [Å] of Fe and C were calculated using Eq. (5) based upon the Bragg peaks of θ_{200}, θ_{211}, θ_{220}, and θ_{002}, θ_{004}, θ_{006}, respectively. The calculation results were showed in Table 3. It is indicated clearly in that table that the Fe and C elements have got positive lattice strains. It means that **e**ither iron, or carbon elements in composites get a homogeneous tensile-strain field. The lattice strains of Fe and C change with the milling time in a different away (Figure 7). Firstly the lattice strains of Fe get a little bit decrease and then increase with milling time. On the other hand, C get an increase in lattice strain firstly, and tend to be a constant on further milling. The constant lattice strain of C will presumably be attained after 5.0 hours milling time.

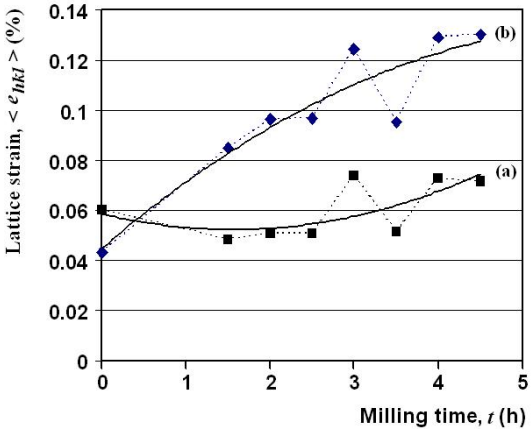

Figure 7. The lattice strains of iron (a) and carbon (b) change with the milling time, t in a different away.

Furthermore, the lattice strains obtained from Equation (4) were used to calculate the residual stress, *ó* using Equation (6), where $<e_{hkl}>$ = *å*. The calculation results are indicated in Table 3. It is clearly showed that the residual stress, *ó* versus milling time, *t* in carbon tends to be constant at about 10 GPa. It might be due to the carbon particles are trapped in between the iron particles and distributed in the ductile matrix of iron. Thus any external disturbances, such as ball colliding, are absorbed by the iron matrix.

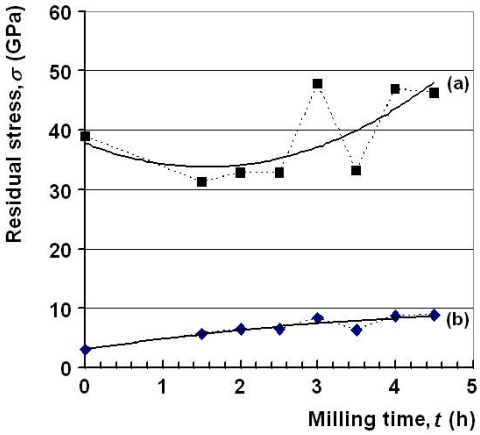

Figure 8. The residual tensile stress, σ versus milling time, t in iron (a) and in carbon (b).

At first there is a stress release in Fe after being milled for 1.5 h. This is because of the Fe crystallites were fractured from 426 ú to 343 ú. But after being milled for 2.0 h, the Fe crystallites were welded and therefore the size of Fe crystallites increased again to be 446 ú and so also its residual stress. On the further milling through 5.0 h, the welding processes continuously occurred. Thus, the crystallites size and the residual stresses of Fe have a tendency to increase as indicated in Table 3 and Figure 8, respectively.

Table 4. Magnetic parameter of Post Milling Fe-C composite

Milling Time (hours)	Coerciv. Magnetic, Hc(Oe)	Saturated Magn., Ms(emu/gram)	Anisotropy Magn., Ku 10^6(erg/cc)	Remanance Magn., Mr (emu/gram)
1,5	100,5	131	0,6582	5,0
4,0	108,5	136	0,7378	7,0

Furthermore, the magnetic properties of the samples can be analyzed from the parameter magnetic taken from M-H curve, as summarized in Table 4.

It is well known that coercivity and anisotropy are closely related. For example, if the reversal of the magnetization takes place by coherent rotation, coercivity and anisotropy should be proportional to each other,i.e., Hc= 2Ku/Ms ,in the Stoner-Wohlfarth model. One explanation the enhancement of the coercivity and anisotropy in the sample post 4,0 hours milling compare to 1,5 hours milling is increasing of the grain size of Fe particles as calculated from RIETAN analysis. This condition increasing the Hc due to a strong exchange coupling between Fe grain.

Edisi Khusus Oktober 2007, hal : 88 - 94
ISSN : 1411-1098

CONCLUSION

Mechanical milling of $Fe_{50}C_{50}$ composites using high energy milling for 4.5 hours result in a better crystallization of the component powders. So, the amorphization of the elemental powders do not happen yet. The carbon elements in $Fe_{50}C_{50}$ magnetic composites get a homogeneous strain field, while the iron elements get an inhomogeneous strain field. The crystallite size of C particles get only a small change until the milling time of 4.5 hours. This is presumably due to the C particles are trapped at the weld interfaces between the Fe particles. While, the Fe particles fracture into smaller segments on the milling time of 1.5 hours. On the further milling, the Fe particles undergo welding processes to be larger crystallites. Magnetic parameter such as Hc, Ms and Ku were confirmed this suggestion.

ACKNOWLEDGEMENTS

We would like to thank to the Head of Technology Centre for Nuclear Industrial Material, Dr. Ridwan and the Head of Composite Nano Group, Nuclear Analysis Division, on their supports; also our thanks to all of our colleagues on their helps. This project has been founded by DIPA-BATAN 2006.

REFERENCES

1. C.Q.JIN, X.WANG, Z.X. LIU, Y.L. ZHANG, F.Y.LI, and R.C.YU, *Brazilian Journal of Physics*, **33** (4) (2003) 723-728
2. D.L. NOVIKOV, V.A. GUBANOV, and A.J. FREEMAN, *Physica* C, **191** (1992) 399-408
3. R. RICARDO DA SILVA, J.H.S. TORRES, and Y. KOPELEVICH, *Phys. Rev. Lett.*, **87** (2001) 14700.
4. Q.Z. XUE, X. ZHANG, and D.D. ZHU, *J. Magnetism and Magnetic Materials*, **270** (2004) 397-402
5. D.S. KUPPERMAN, S. MAJUMDAR, and J.P. SINGH, *Neutron News*, **2** (3) (1991) 15-18
6. XUN-LI WANG, CAMDEN R. HUBBARD, KATHLEEN B. ALEXANDER, PAUL F. BECHER, JAIME A. FERNANDEZ-BACA, and STEVE SPOONER, *J. Am. Ceram. Soc.*, **77** (6) (1994) 1569-1575
7. R.J. HILL and C.J. HOWARD, *J. Appl. Crystallogr.*, **20** (1987) 467-474
8. H.P. KLUG and L.E. ALEXANDER, *X-ray Diffraction Procedures*, **2**nd Ed; Wiley, New York, (1974) 618-708
9. G. CAGLIOTTI, A. PAOLETTI, and F.P. RICCI, *Nuc. Instrum.*, **3**, (1958) 223-228
10. http://amialabs.com/AppNoteC02.swf, 26 June 2006
11. ENGKIR SUKIRMAN dan WISNU ARI ADI, *J. Sains Materi Indonesia*, **Edisi Khusus Oktober 2006** (2006) 147-153
12. http://www.engineering.usu.edu/mae/faculty/stevef/info/MProp/Iron_ASTM_A47-A. htm, June 19, 2007.
13. COST JAMES R., JANOWSKI KENNETH R., ROSSI RONALD C., *J. Nuclear Materials*, **225** (1995) 267-272
14. C.C. KOCH and J.D. WHITTENBERGER, *Intermetallics*, 4 (1996) 339-395
15. F. IZUMI, *Rigaku J.*, **6**, 10 (1989)